Nocturnal Light Environments and Species Ecology: Implications for Nocturnal Color Vision in Forests

Carrie C. Veilleux*[1] and Molly E. Cummings[2]

[1]Department of Anthropology, University of Texas at Austin, Austin, TX 78712
[2]Section of Integrative Biology, University of Texas, Austin, TX 78712, USA

*Corresponding Author:
Carrie C. Veilleux
Department of Anthropology
University of Texas at Austin
1 University Station C3200
Austin, TX 78712-0303
Phone: (512) 203-9760
Fax: (512) 471-6535
carrie.veilleux@utexas.edu

Running Title: Nocturnal Light Environments

Key Words: visual ecology, nocturnal color vision, light environments, rainforest, dry forest

Summary

While variation in the color of light in terrestrial diurnal and twilight environments has been well documented, relatively little work has examined the color of light in nocturnal habitats. Understanding the range and sources of variation in nocturnal light environments has important implications for nocturnal vision, particularly following recent discoveries of nocturnal color vision. In this study, we measured nocturnal irradiance in a dry forest/woodland and a rainforest in Madagascar over 34 nights. We found that a simple linear model including additive effects of lunar altitude, lunar phase and canopy openness successfully predicted total irradiance flux measurements across 242 clear sky measurements (r = 0.85; p<0.0001). However, the relationship between these variables and spectral irradiance was more complex, as interactions between lunar altitude, lunar phase and canopy openness were also important predictors of spectral variation. Further, in contrast to diurnal conditions, nocturnal forests and woodlands share a yellow-green-dominant light environment with peak flux at 560 nm. To explore how nocturnal light environments influence nocturnal vision, we compared photoreceptor spectral tuning, habitat preference and diet in 32 nocturnal mammals. In many species, long-wavelength-sensitive cone spectral sensitivity matched the peak flux present in nocturnal forests and woodlands, suggesting a possible adaptation to maximize photon absorption at night. Further, controlling for phylogeny, we found that fruit/flower consumption significantly predicted short-wavelength-sensitive cone spectral tuning in nocturnal mammals (p=0.002). These results suggest that variation in nocturnal light environments and species ecology together influence cone spectral tuning and color vision in nocturnal mammals.

Introduction

Recent discoveries of functional color vision at low light levels among nocturnal geckos, tree frogs, bees and hawkmoths (Kelber et al., 2002; Roth and Kelber, 2004; Somanathan et al., 2008; Gomez et al., 2010) have prompted a re-evaluation of the importance of color vision for nocturnal animals. Traditionally, the low light intensities available in nocturnal environments were believed to preclude color discrimination (Walls, 1942; Ahnelt and Kolb, 2000). Recent studies, however, suggest that nocturnal color vision may be both selectively advantageous for some species and more widespread than previously believed (Kelber and Roth, 2006; Gomez et al., 2009; Müller et al., 2009). Color discrimination at nocturnal light levels may even be adaptive for some mammals. Studies of opsin genes in nocturnal primates and bats, for example, have revealed evidence of selection acting to maintain functional dichromacy in several lineages, possibly for nocturnal color discrimination (Kawamura and Kubotera, 2004; Perry et al., 2007; Zhao et al., 2009a,b). Further, recent work suggests that cone thresholds in some nocturnal mammals may extend down to dim moonlight or starlight levels (Umino et al., 2008). Because the appearance of visual targets (such as conspecifics, food, or predators) depends upon the spectral quality of ambient light as well as the target's reflective properties (Endler, 1990; Endler, 1993), an understanding of the light environments available to nocturnal animals may be instrumental in studying nocturnal color vision (Johnsen et al., 2006).

Endler's (1993) seminal work "The Color of Light in Forests and Its Implications" offered a detailed study of variation in diurnal light environments, forming the basis for most subsequent work on diurnal visual ecology. In contrast, variation in nocturnal light environments has not been as extensively studied. By "nocturnal light environments," we are referring strictly to the nocturnal period after the conclusion of twilight (for twilight environments, see: Munz and McFarland, 1973; Munz and McFarland, 1977; Martin, 1990; Endler, 1991; Endler, 1993; Lee and Hernandez-Andres, 2003; Johnsen et al., 2006; Sweeney et al 2011). Much of the published research on nocturnal light environments has focused on variation in light intensity. These studies reveal that light intensity at night can vary dramatically, differing by as much as eight orders of magnitude due to lunar phase, lunar altitude (height of the moon in the sky), weather, foliage density, seasonality and latitude (US Navy, 1952; Lythgoe, 1979; Pariente 1980; Martin, 1990; Cummings et al., 2008; Warrant, 2008; Johnsen, 2012).

However, few data are currently available on spectral variation in light environments at night. Munz and McFarland (1973; 1977) and Lythgoe (1972; 1979) identified spectral differences between moonlight and starlight. While the spectral quality of moonlight resembles sunlight, starlight is "red-shifted," with maximum irradiance displaced to longer wavelengths (Lythgoe, 1972, 1979; Munz & McFarland, 1973, 1977). Pariente (1980) identified spectral variation between lunar phases in his study of moonlight inside and outside forests in Madagascar. He found that quarter moonlight is relatively richer in wavelengths greater than 750 nm (i.e. "redder") compared to full moonlight, consistent with astronomical studies of lunar irradiance and lunar surface reflectance (Lane and Irvine, 1973; Kieffer and Stone, 2005). More recently, Johnsen et al. (2006) examined nocturnal spectral irradiance under conditions ranging from clear full moon sky in an open environment to urban locations under overcast moonless sky, with an emphasis on how these spectra differ from diurnal and twilight conditions. Their findings support previous work—under full moonlight, the spectrum was "nearly indistinguishable" from daylight, while their modeled starlight was red-shifted (Johnsen et al., 2006). Thus, current evidence suggests nocturnal light environments can vary with lunar phase, foliage density (Lythgoe, 1972; Pariente, 1980) and cloud cover (Munz and McFarland, 1973). However, a systematic study of how these variables (as well as lunar altitude) influence nocturnal light in natural forest habitats is currently lacking.

Studies of aquatic and diurnal terrestrial visual ecology have frequently linked photoreceptor types, photoreceptor spectral tuning or visual signaling morphology (e.g. dewlap or plumage coloration) with the spectral quality of ambient light environments (Munz and McFarland, 1973, Lythgoe, 1979; Lythgoe, 1984; Endler, 1991; Endler, 1993; Endler and Théry, 1996; Chiao et al., 2000; Théry, 2001; Cummings and Partridge, 2001; Leal and Fleishman, 2002; Cummings, 2007). In contrast, research examining the relationships between nocturnal light environments, nocturnal visual morphology and behavior has been relatively limited (e.g., Osorio and Vorobyev, 2005; Johnsen et al., 2006; Melin et al., 2012). Nocturnal environments can be extremely photon-limited, exhibiting light levels that are five to nine orders of magnitude darker than daylight (Munz and McFarland, 1973; Lythgoe, 1979; Pariente, 1980). Animal visual systems only encode a fraction of the photons reaching the cornea (~55-59% in invertebrates, 5-25% in vertebrates), with photons lost at both absorption and transduction stages (Barlow et al., 1971; Lillywhite, 1977; Warrant, 2004). Consequently, nocturnal animals may experience strong

selective pressure to maximize photon absorption by tuning photoreceptor spectral sensitivities to the dominant wavelengths of ambient light in their preferred habitats, similar to that seen in aquatic animals (Lythgoe, 1984; Partridge and Cummings, 1999; Cummings and Partridge, 2001). Additionally, changes in the spectral quality of ambient light can have a large effect on the reflectance and visibility of targets (Johnsen et al. 2006; Kelber & Roth 2006). If nocturnal habitats vary substantially in photon abundance at different wavelengths, nocturnal animals from different habitats may be expected to differ in peak cone spectral sensitivities.

In this study, we had three objectives: (1) to describe the range of variation in nocturnal light environments present in woodlands and forests in Madagascar, (2) to identify factors affecting intensity and spectral variation in nocturnal light environments within these habitats and (3) to explore ecological factors that may influence visual pigment spectral tuning in nocturnal vertebrates. We first measured nocturnal irradiance over 32 nights at multiple locations in an open canopy dry forest/woodland and 2 nights in a closed canopy rainforest. From these data, we examined the effects of lunar phase, lunar altitude and canopy openness on nocturnal spectral irradiance using spectral comparisons and linear mixed effects modeling. Finally, we compared photoreceptor spectral sensitivities for 40 nocturnal vertebrates with different habitat preferences and diets to further examine the relationship between nocturnal light environments, ecology and vision.

MATERIALS AND METHODS

Study sites

Research was conducted at two forests in Madagascar representing different habitat types: Kirindy Mitea National Park and Ranomafana National Park. Kirindy Mitea is an open canopy dry deciduous forest/succulent woodland habitat (Burgess et al., 2004). Data were collected exclusively at the Ankoasifaka (Anko) Research Station (20º 47.25’ S, 44º 10.14” E) between July and September 2009. This period represents the end of the dry season when the majority of tree species have dropped their leaves (Sorg and Rohner, 1996) and thus would be expected to show the greatest contrast with closed canopy rainforests. Although Anko has no history of systematic logging, a cyclone struck the forest in January 2009 that was found to affect forest structure compared to pre-cyclone conditions (Lewis and Bannar-Martin, 2012). However, a comparison of tree size classes revealed that forest structure at Anko did not significantly differ

from that of other dry forests in Madgascar (Veilleux, unpublished). Ranomafana is a humid rainforest with lowland to montane forest habitats (Wright, 1992). Data were collected at the Valohoaka (Valo; 21º 17.76' S, 47º 26.35' E) and Talatakely (Tala; 21º 15.75' S, 47º 25.25' E) research sites in September and October 2009. Valo (1200 m elevation) is undisturbed primary forest (Balko and Underwood, 2005). Tala (500 m elevation) experienced logging in the late 1980s and is characterized as secondary rainforest (Wright, 1992).

Foliage density measurements

At all sites, nine 50 m transects were established 3-10 m parallel to trail systems. At 3 m distance, the trail was not visible and so had no effect on measurements of foliage density. Foliage density was measured at 10 m intervals along each transect using hemispheric photography. Photographs were taken with a Nikon Coolpix 5700 digital camera and FC-E9 Nikon fisheye lens positioned on a tripod (0.89 m height). Foliage density was quantified as percent canopy openness calculated from digital photographs in Gap Light Analyzer v.2.0 (Frazer et al., 1999). In the dry forest site at Anko, canopy openness ranged from 19 to 50% open, with a median canopy openness at 38%. By contrast, canopy openness in the rainforest ranged from 13 to 26% open (medians: Valo-16%, Tala-20%).

Nocturnal irradiance measurements

We collected 532 nocturnal irradiance measurements, including 514 measurements from Anko, 8 from Valo and 10 from Tala. All measurements were collected using an International Light (Peabody, MA, USA) IL1700 research radiometer and calibrated PMC271C photomultiplier detector (200-675 nm sensitivity range) positioned on a tripod (0.89 m height) with 12 narrow-bandpass interference filters (Newport Oriel Corporation, Irvine, CA, USA) positioned in a filter wheel resting on the detector. The filters had central wavelengths across the visible spectrum, full-width half maximum wavelengths of 10±2 nm, and minimum peak transmission of 30-50%. Filter model numbers were 10BPF10- 400 nm, 10BPF10- 420 nm, 10BPF10- 430 nm, 10BPF10- 440 nm, 10BPF10- 460 nm, 10BPF10- 490 nm, 10BPF10- 520 nm, 10BPF10- 540 nm, 10BPF10- 560 nm, 10BPF10- 580 nm, 10BPF10- 620 nm and 10BPF10- 650 nm. Due to technical error, an additional filter (680 nm central wavelength, model #10BPF10- 680 nm) was used in place of the 650 nm filter for 90 full moon measurements at Anko. As a result, some comparisons include those 680 nm measurements. Total flux was directly measured by the IL1700 and PMC271C without any filter and recorded as the average of two measurements taken

consecutively. Using a LI-COR Spectral Irradiance Lamp (1800-02L) and a series of neutral density filters (one Edmund Optics 2.0 NDF, one Oriel 1.0 and two Lee 0.6 NDF filters), we calibrated the IL1700 with each of the 13 interference filters in order to convert $W/cm^2/s$ photomultiplier units into photometric units (micromoles or μM of photons; $\mu M/m^2/s/nm$).

During measurement, the photomultiplier detector was pointed directly up at the sky (90° zenith angle) and researchers crouched below the height of the detector. Cloud cover was assessed by whether any clouds were detected when looking directly overhead ("clear" or "cloudy"). We had no means to quantify the degree of cloudiness, so we restricted most analyses of nocturnal irradiance to clear skies. However, the sky was completely overcast for three measurements at Anko, so we could compare the same three measurement locations under clear sky and complete cloudiness. The time of data collection varied nightly but always began after astronomical twilight had ended (i.e., when the sun no longer contributes to nocturnal irradiance; Martin, 1990), as determined for the latitude and longitude of the study site (USNO, 2011). At Anko and Valo, measurements occurred between 19:18 h and 00:52 h. At Tala measurement occurred between 23:51 h and 04:00 h. Using the time/date of measurement and the latitude/longitude of the study site, the position of the moon in the sky (lunar altitude) and the fraction of the lunar face illuminated (lunar fraction) were determined for each measurement from data available at the United States Naval Observatory (USNO, 2011). At Anko, nocturnal irradiance was measured over 32 nights (29 July - 8 Sept 2009). Data were collected at 10 m intervals along the nine botanical transects (54 measurement location). Each measurement location was revisited approximately every 4 nights to sample locations across a lunar cycle. At Valo and Tala, nocturnal irradiance was measured on one night each. At Tala, data were collected for 10 measurement locations on a gibbous moon night (8 Oct 2009, 3 clear, 7 cloudy). At Valo, data were collected at 12 locations on a clear crescent moon night (22 Sept 2009). However, four locations at Valo were excluded from analysis because irradiance was too low to measure with spectral filters.

Nocturnal irradiance analyses

We constructed nocturnal irradiance spectra for each observation by combining the 12 filter measurements (in photometric units ($\mu M/m^2/s/nm$) and explored how lunar phase, lunar altitude, canopy openness, cloud cover and habitat type influenced spectral and intensity features of nocturnal light environments. We restricted most comparisons within the dry deciduous forest at

Anko to clear sky conditions (*n*=347 measurements). Lunar fractions were grouped into lunar phases: crescent (0.01-0.39), quarter (0.40-0.69), gibbous (0.70-0.90), full (0.91-1.0). To compare the influences of these factors on the shape of the spectra independent of total flux, we normalized each observation spectrum to its own maximum flux. We then calculated the mean and standard error in subsets of the spectra under different conditions for each filter wavelength. Because there was sometimes variation between spectra at the wavelength of peak flux, this method depicts the degree of variation in spectral shape within subsets (i.e. whether the mean peak flux in a condition equals 1 or is more variable).

We also sought to quantify the effects of these factors (lunar phase, lunar altitude, canopy openness) on nocturnal irradiance (both intensity and spectral characteristics) using linear mixed effects modeling. We restricted analyses to subsets of data representing clear sky observations at Anko (moonlight=242 measurements, no moon=99 measurements). We defined nocturnal light in terms of total flux (in W/cm^2, as measured directly by the IL1700 and PMC271C without any filter) as well as proportional flux across different bandwidths (short-wavelengths, %SW: 400-460 nm; middle wavelengths, %MW: 490-540 nm and long wavelengths, %LW: 560-650/680 nm). The spectral variables (%SW, %MW and %LW) were calculated from raw measurements (W/cm^2) taken with the relevant filters (i.e. 400-460 for %SW) divided by the sum of measurements from all filters. We chose the spectral bandwidths to correspond to typical categories of mammalian visual pigments (S: 400-460 nm, M: 510-540 nm, L: >540 nm; Jacobs, 2009). For these data, we transformed lunar fraction to a measure of “lunar phase angle”, where 0 is full moon (fraction=1.0) and 180° is new moon (fraction=0). Because lunar irradiance exhibits a nonlinear relationship with lunar phase angle (Miller and Turner, 2009; Johnsen, 2012), we interpolated the lunar phase function for each lunar phase angle using lunar phase function values at 501.2 nm from Miller and Turner (2009). Lunar altitude was also cosine-transformed for each measurement. We designated measurement location and transect as nested random effects (locations nested within transects) to prevent spatial and temporal autocorrelation.

We had no *a priori* expectations regarding the relative importance of interactions between the factors (cosine lunar altitude, lunar phase function, and canopy openness). Therefore, we ran the full set of possible models (including all interactions) for each nocturnal irradiance variable using the *lme4* package (Bates and Maechler, 2010) in R v.2.12.2 (R

Development Core Team, 2011). For each model, we used maximum likelihood estimates to determine the Akaike Information Criterion (AIC). We then calculated ΔAIC (the difference in AIC between the best model and each of the other models), evidence ratios, and Akaike weights for the models of each nocturnal irradiance variable following Symonds and Moussalli (2011). In general, models with ΔAIC < 2 are considered "almost as good" as the best model, while ΔAIC > 9 have relatively little to no support (Burnham and Anderson, 2004; Burnham et al., 2011; Symonds and Moussalli, 2011). Evidence ratios and Akaike weights are alternative measures of the relative model strength that estimate how much better the best model fits the data compared to the given model and the probability that the given model is the best of competing models, respectively (Burnham and Anderson, 2002; Burnham and Anderson, 2004; Symonds and Moussalli, 2011). We also calculated the relative importance of each factor/interaction by summing the Akaike weights of all models including that factor/interaction (Burnham and Anderson, 2002). This factor weight reflects the probability that the factor/interaction is a component of the best model (Symonds and Moussalli, 2011). We chose the model with the lowest AIC value for each nocturnal irradiance variable and reran the model with restricted maximum likelihood estimates to determine the model parameters. For variables where multiple models had ΔAIC < 2, we utilized the simplest model (fewest number of terms). We then evaluated how well the model predicted each nocturnal irradiance variable by comparing estimates predicted by the best model to that observed in the dataset.

Nocturnal vertebrate visual pigments

From the published literature, we compiled a dataset of known visual pigment peak spectral sensitivities (λ_{max}), habitat preferences and diet for 40 nocturnal vertebrates across a variety of taxonomic and ecological groups (Table 1 in supplemental materials). Visual pigment spectral sensitivities were grouped into three categories based on typical mammalian photoreceptor pigment classes (Jacobs, 2009): rods, short-wavelength-sensitive (SWS) cones (including ultraviolet sensitivity: UV), and medium to long-wavelength-sensitive (LWS) cones. We restricted statistical analyses of cone pigments to placental and marsupial mammals in order to limit phylogenetic effects on spectral tuning. Most vertebrates possess four cone pigment (opsin) genes (*SWS1, SWS2, Rh2,* and *LWS*) that produce different classes of cones, including two types sensitive to shorter wavelengths (355-470 nm) and two sensitive to middle and longer wavelengths (480-570 nm; Hunt et al., 2009). In contrast, mammals have an evolutionary history

of nocturnality that resulted in the shared loss of *SWS2* and *Rh2* genes (Jacobs and Rowe, 2004; Hunt et al., 2009). Consequently, most nocturnal mammals have only two cone classes (SWS and LWS) derived from homologous genes (*SWS1* and *LWS*, respectively), which allows a more controlled comparison of ecological effects on spectral tuning.

We used a phylogenetic generalized least squares (PGLS) approach to explore the association between habitat type and dietary composition with SWS and LWS spectral tuning in nocturnal mammals (*n*=32 species). PGLS utilizes known taxonomic relationships and branch lengths to compensate for the influence of phylogeny on trait covariation (Garland and Ives, 2000). For each species, we categorized habitats as "open canopy/woodland" (including seasonally open forests, forest edges), "closed canopy" (including rainforests, cloud forests), "open/closed canopy" (if a species is present in both types), and "open" if savannah/desert. One primate (*Cheirogaleus medius*), while inhabiting seasonally open canopy deciduous forests, hibernates through the dry season and is only active in the rainy season, when the forest has a closed canopy (Fietz and Ganzhorn, 1999). This species was thus included in the "closed canopy" habitat group. We restricted PGLS analyses to species from "open canopy/woodland" or "closed canopy" habitats, excluding those from both habitats ("open/closed"). We also categorized each species depending on whether it included fruit or flower products, which advertise visually to consumers, as 10% or more of its diet (Y/N). Dietary data were collected from studies of feeding time, fecal content, or gut content (see Table S1 for references).

We utilized phylogenetic and branch length data from a published mammalian supertree (Bininda-Emonds et al., 2007). PGLS analyses were performed in R using *ape* (Paradis et al., 2004), *caper* (Orme et al., 2010) and *geiger* (Harmon et al., 2008) packages. We conducted separate PGLS for habitat and diet categorical factors, excluding taxa with missing values. Trees used for each analysis are presented in Figure 1 in supplemental materials. For each comparison, we also calculated Pagel's lambda, which measures the effect of phylogeny in the data, where 0 reflects no phylogenetic influence and 1 reflects a strong phylogenetic signal (Pagel, 1999, Kamilar et al., 2012). We also excluded one species (*Phodopus sungorus*) because it has SWS and LWS pigment co-expression (both pigments present in a single cone) in all cones and no functional color vision (Lukáts et al., 2002). While most mammals are dichromats (having two cone types) one nocturnal marsupial (*Setonix brachyurus*) has three cone types (Cowing et al., 2008), two of which are categorized as medium/long-wavelength-sensitive (502 nm and 538

nm). To account for this second cone type in PGLS analyses involving LWS pigments, *Setonix brachyurus* was represented by two branches (branch length set at 0.0001).

RESULTS

Variation in nocturnal irradiance: effects on total light intensity

Comparisons of absolute spectra reveal that total light intensity in the open canopy dry forest at Anko varied substantially under different nocturnal conditions. The most dramatic variation in intensity was found with changes in lunar phase (Fig. 1A,B) and lunar altitude (Fig. 2A). Average flux at 560 nm, for example, was 182 times brighter under a full moon compared to no moon, and 7.9 times brighter than under a quarter moon. Similarly, 560 nm-flux under a full moon at high lunar altitudes (60-90°) was 48 times brighter than that at low lunar altitudes (0.1-29.9°). Canopy openness (Fig. 3A-C) and cloud cover (Fig. S2) also influenced light intensity at measurement locations within Anko, albeit to a lesser degree. Further, the impact of canopy openness on nocturnal light intensity was influenced by lunar altitude (Fig. 3A-B). Under a full moon, more open canopy measurement locations (>45% open) were 4.4 times brighter than more closed locations (<30% open) for average 560 nm-flux at higher lunar altitudes, but only 0.5 times brighter at lower lunar altitudes. When the moon was absent, open canopy locations were 1.5 times brighter than closed locations (Fig. 3C). Cloud cover appeared to have the smallest impact on light intensity (Fig. S2).

To quantify the effects of lunar phase function, cosine lunar altitude and canopy openness on nocturnal irradiance, we ran linear mixed models on 242 clear sky moonlight observations at the dry forest site of Anko. The factor weights for each potential model term are presented in Table 1, while model comparisons (AIC, ΔAIC, evidence ratios, Akaike weights) are summarized in Table S2. The best model explaining variation in log total flux was the simple main factor additive model:

$$LogTotalFlux = -9.121 - 2.11A + 0.822P + 1.627C$$

Where A is cosine lunar altitude, P is lunar phase function, and C is fraction canopy openness (model parameters and factor p-values: Table S3). The log total flux values predicted by this model were strongly correlated (r=0.85, p<0.0001) with observed values at Anko (Fig. 5A), although the model was not as good at prediction at higher light intensities. Values predicted by

this model for the rainforest measurements were also significantly correlated with observed rainforest log total flux, r=0.61, p=0.007 (Fig. 5A), despite small rainforest sample size (n=18) and cloud cover. Comparisons of models and model weights indicates that lunar altitude had the strongest effect (Table S2), as exclusion of this factor resulted in a ΔAIC = 268.8, suggesting the best model was more than 70 billion times better supported (Burnham et al., 2011). By contrast, ΔAIC for the highest ranked model excluding lunar phase function was 73.4, while that excluding canopy openness was only 7.1 (Table S2). Interactions between the main factors (altitude, phase and canopy) appear to play a minor role in predicting nocturnal intensity, as the factor weights for these interactions were relatively low (Table 1). Interestingly, linear mixed model estimations for nocturnal intensity under starlight at Anko (n=99 measurements; with canopy openness as the factor) did not have as strong explanatory power. Although canopy openness was significantly related to log total flux (Table S3), the correlation between predicted and observed values under starlight were not as strong as under moonlight, r=0.50, p<0.0001. Canopy openness thus explained only 25% of the variation in log total flux when the moon was not present.

Variation in nocturnal irradiance: effects on spectral quality

While total intensity varied greatly under different nocturnal conditions, spectral irradiance measurements reveal that the wavelength of maximum flux (560 nm) was relatively consistent across most conditions, microhabitats, and habitat types (Figs 1-4, S2), suggesting that light environments in nocturnal forest and woodlands generally resemble Endler's (1993) yellow/green-rich *forest shade* light environment. However, lunar phase, lunar altitude, canopy openness and cloud cover all exhibited some influence on the nocturnal spectral distribution in the dry forest/woodland at Anko (Figs 1-3, S1). In general, the spectra from full and quarter moons were richer in shorter and middle wavelengths (430-540 nm) compared to "no moon" conditions (Fig. 1C). Spectra under "no moon" conditions were slightly richer in the longest wavelengths measured (650 nm) than moonlight (Fig. 1C), as would be expected considering the "red-shift" of starlight (Lythgoe, 1979; Johnsen et al., 2006). Controlling for lunar phase, light environments from lower lunar altitudes (<60°) were richer in shorter and middle wavelengths (430-560 nm) compared to those when the moon was high in the sky (Fig. 2B). Additionally, as with light intensity, lunar altitude influenced the effect of canopy openness on nocturnal irradiance spectra. While light environments from more open microhabitats at Anko (>30%

open) were richer in shorter and middle wavelengths (430-540 nm) compared to more closed microhabitats (<30% open) when the moon was low in the sky, this variation was reduced at higher lunar altitudes (Fig. 3D,E). Under starlight, closed microhabitats deviated from the green-rich night sky of more open locations with a spectral irradiance peak at 650 nm (Fig. 3C,F).

While the simplest linear mixed model was the best for explaining variation in log total flux in clear moonlit skies, the best-fit models for the spectral quality aspects of nocturnal irradiance (%SW:400-460 nm, %MW: 490-540 nm, %LW: 560-650/680 nm) were more complex. For both %SW and %LW, the best models included interactions between cosine lunar altitude and lunar phase function and cosine lunar altitude and canopy openness (Tables 1, S2):

$$\%SW = 52 - 24.33A - 5.67P - 30.04C + 17.62AP + 65.34AC$$
$$\%LW = 12.59 + 25.64A + 8.89P + 22.01C - 19.48AP - 53.44AC$$

(model parameters and *p*-values: Table S3). Although several models were close in AIC for %MW, the best model was the most complex, including interactions between all main factors:

$$\%MW = 53.35 - 23.61A - 39.77P - 36.68C + 48.08AP + 91.18AC + 43.63PC - 114.73APC$$

In addition to being more complex, the spectral quality models were also less explanatory than the log total flux model (Fig. 4). The model for %SW performed best of the spectral variables (r=0.65, Fig. 4B), followed by %LW (r=0.56, Fig. 4D) and %MW (r=0.48, Fig.4C). For the rainforest dataset, the models generally performed poorly in predicting spectral distribution. For both %SW and %MW, correlations for predicted and observed values were not significant, r=0.25, p=0.31 and r=0.25, p=0.32, respectively. The %LW model performed much better, r=0.61, p=0.008. Similar to the results of moonlight analyses, the models for spectral quality in starlight (Table S3) had relatively low explanatory power. The strength of the correlations for observed and expected values of %SW (r=0.61, df=97, p<0.0001) and %LW (r=0.55, df=97, p<0.0001) were similar to those of moonlight models (Fig. 5B,D), but were worse for %MW values (r=0.36, df=97 p=0.0002).

Variation in nocturnal irradiance: effects of habitat type

Comparisons of nocturnal spectra between the dry forest/woodland at Anko and the rainforest sites (Valo and Tala) suggest habitat differences in nocturnal light environments (Fig. 5). Absolute nocturnal irradiance at both rainforest sites was substantially lower than at Anko

(Fig. 5A,B). In particular, absolute irradiance in the rainforest in crescent moonlight (with lunar altitudes of 6.4 to 28.5°; Fig. 5A) was even lower than starlight irradiance in the dry forest (Fig. 1B). In crescent moonlight (Fig. 5C), the dry forest was substantially richer in shorter and middle wavelengths (420-520 nm) while the rainforest was richer in the longest wavelength measured (650 nm). Similarly, in gibbous moonlight (Fig. 5D), the dry forest was richer in shorter and middle wavelengths (420-560 nm) while the rainforest was richer in longer wavelengths (580-650 nm). Some of this variation between habitats may be due to differences in canopy openness, as all of the dry forest spectra in these comparisons were from relatively open canopied locations (> 37% canopy openness) compared to Valo (14 to 21.3%) and Tala (15 to 22%). The spectra from the rainforest sites resemble that of more closed canopy Anko locations (Fig. 3) in lacking a secondary peak at 490 nm. However, in contrast to the closed canopy Anko locations under moonlight, both rainforest sites both exhibited an increase in the longer wavelengths at 650 nm. This increase in the longer wavelengths in the closed canopy rainforest sites resembles that seen in starlight at Anko closed canopy locations (Fig. 3C,E).

Ecological effects on nocturnal visual pigments

In our comparison of nocturnal vertebrate visual pigments (Table S1, Fig. 6), we found that rod λ_{max} is fairly constant (498-507 nm) across major groups. However, there was substantial variation in cone pigment λ_{max}. We found a wide range of SWS cone λ_{max} in nocturnal vertebrates (358-467 nm). In particular, ultraviolet-sensitive SWS cones (358-366 nm) were very common among nocturnal mammals and reptiles. Among mammals, SWS cone loss was also fairly common across taxonomic groups (Fig. 6). In contrast to SWS cones, the range of λ_{max} for LWS cones (502-562 nm) was more limited. Additionally, while most species had either one or two cones, several had three cones (particularly non-mammals), raising the possibility of trichromatic nocturnal color vision in several vertebrate groups (Fig. 6).

PGLS analyses identified a strong phylogenetic signal in mammalian SWS and LWS spectral tuning (Table 2). Despite a strong influence of phylogeny, we still detected a significant effect of fruit/flower consumption on mammalian SWS λ_{max} (Table 2, Fig. 6). This result suggests that in our small sample of nocturnal mammals (n=31), controlling for phylogeny, species that include fruit or flower products as >10% of their diets had SWS cones tuned to shorter wavelengths than those that do not. In contrast, habitat type (open canopy forest *vs.* closed canopy forest) had no effect on SWS spectral tuning. Similarly, both diet and habitat type

did not influence LWS pigment spectral tuning in our nocturnal mammal sample. Interestingly, in the LWS analysis for habitat, there was no phylogenetic signal (lambda=0) for the habitat subset of species (Table 2, Fig. S1).

DISCUSSION

Effects on variation in nocturnal irradiance in Madagascar

Measurements of the Malagasy night sky revealed that the total intensity of nocturnal light varies significantly both spatially over the landscape (canopy openness) and temporally over a night (lunar altitude), month (lunar phase) and year (dry vs wet season). Consistent with previous research, lunar phase exhibited the strongest influence on the total intensity of nocturnal light when comparing full moon *vs.* no moon present (Lythgoe, 1979; Pariente, 1980; Warrant, 2004; Johnsen et al. 2006; Warrant, 2008). However, once the moon was up, the height of the moon in the sky actually exhibited a much stronger effect on total intensity than lunar phase or canopy openness. While other researchers have documented an effect of lunar altitude on light intensity (e.g. Bidlingmayer 1964; Young and Mencher, 1980; Martin, 1990; Johnsen, 2012), to our knowledge, this is the first study to quantify the relative significance of lunar altitude on variation in nocturnal light intensity in natural forest environments. Further, we discovered that a simple additive model of the effects of lunar altitude, lunar phase, and canopy openness on total flux had strong predictive power in clear moonlit skies. The lower predictive power of the model for starlight conditions (only including canopy openness as a factor) may be due to the effects of other influences on intensity in moonless nights, such as zodiacal light or airglow (Johnsen, 2012).

In contrast to the dramatic changes in total intensity, the spectral quality of nocturnal irradiance was fairly constant across most conditions, exhibiting a yellow-green-dominant light environment with a peak flux at 560 nm. These nocturnal spectral irradiance measurements differed from those collected in non-forested regions in other geographic areas that do not show a dominant peak at 560 nm for moonlit nights (McFarland et al., 1973; Johnson et al., 2006; Melin et al., 2012). The dominant yellow-green spectral irradiance of nocturnal skies in Malagasy forests under both moonlit and moonless nights suggests that the surrounding green foliage in these habitats may have a significant influence on spectral irradiance. Our findings diverge from observations in diurnal forests (Endler, 1993), which identified substantial variation

in peak flux with canopy openness (e.g. blue-rich *woodland shade vs.* green-rich *forest shade*). Instead, regardless of lunar altitude, lunar phase, moon presence or canopy openness, most measurements in both the open canopy dry forest/woodland and closed canopy rainforest shared a spectral distribution similar to that of the green *forest-shade* conditions in diurnal terrestrial forests (Endler, 1993). The difference between nocturnal and diurnal forest light environments (particularly the dropout of shorter wavelengths in nocturnal open canopy woodland environments and constant 560-nm flux across nocturnal conditions) may be due to the significant variation in the intensity of light sources by day and by night. By day, the intensity of the blue sky (which is a major contributor to the blue-dominant open canopy *woodland shade* environments) is five orders of magnitude dimmer than sunlight, but still an order of magnitude brighter than vegetation (Endler, 1993). While the effect of Rayleigh scattering is comparable between moonlight and sunlight (resulting in similar blue skies: Shaw, 2005), full moonlight is 5-6 orders of magnitude dimmer than sunlight (Lythgoe, 1979; Pariente, 1980; Warrant, 2008). Hence, the contribution of blue skies to forest light environments is likely to be reduced under nocturnal conditions, although possibly still relevant for nocturnal animals with highly sensitive visual systems, such as hawkmoths (Kelber et al., 2002).

While the much dimmer intensity of nocturnal light sources resulted in a shared light environment across nocturnal woodlands and forests, comparisons of spectra and bandwidth (%SW, %MW, %LW) modeling still identified spectral effects of lunar altitude, lunar phase and canopy openness within this broad yellow-green dominant environment. Many of these effects are comparable to those seen diurnally, albeit at a much lower magnitude. By both day and night, for example, increased canopy openness is associated with relative increase in shorter wavelengths (day: Endler, 1993). Similarly, lower lunar or solar altitudes generally result in a relative enrichment in shorter wavelengths (day: Condit and Grum, 1964). The models for predicting spectral quality were complex, involving multiple interactions, and had reduced predictive power compared to that for total flux. Yet as with total flux, the models for moonlit skies revealed that lunar altitude was one of the most important factors for spectral variation (both as a main effect and in interaction with lunar phase and canopy openness), suggesting again that lunar altitude may be more important for understanding nocturnal light environments than previously identified.

Target detection and spectral tuning in nocturnal light environments

Of the 32 nocturnal mammals sampled, 10 were monochromats (possessing only LWS cones), 21 were dichromats (possessing both LWS and SWS cones), and 1 was a trichromat (possessing two LWS cone types and SWS cones). Whether monochromat, dichromat, or trichromat, most of the nocturnal mammals in this survey exhibited LWS λ_{max} values clustered around 550 nm, which is near the peak flux we identified in nocturnal woodland and forest habitats (Fig. 6). We observed no significant variation among mammals in SWS or LWS cone λ_{max} with habitat type, which is not surprising given that lack of measured spectral variation in nocturnal irradiance based on canopy cover or habitat type (Fig. 3,5). Some researchers have predicted that λ_{max} should be lower in animals using cones in dim light in order to minimize noise caused by thermal isomerization (Osorio and Vorobyev, 2005). However, the match between LWS λ_{max} and nocturnal light environment suggests that many nocturnal mammals may be tuning their LWS visual pigments to maximize photon absorption to the ambient light available at night. This is not unlike many dichromatic fish that inhabit intensity-limited environments and contain LWS cones tightly matched to the sidewelling irradiance spectrum (Levine and MacNichol, 1979; Bowmaker et al., 1994; Cummings and Partridge, 2001). Unfortunately, the limited data available for other nocturnal vertebrate groups prevents discussion of ecological effects on nocturnal bird or lizard visual pigments.

While the LWS cones in many nocturnal mammals exhibit apparent spectral tuning for the dominant light field characteristics of nocturnal forests, the SWS cones of the nocturnal mammals in this study exhibited a strong association with foraging target. Although sample size was fairly low, our phylogenetically-corrected analyses revealed that nocturnal mammals that consume fruit or flower products have shorter SWS cone λ_{max} values than those that do not (Fig. 6). This foraging target-dependent variation in SWS λ_{max} values among nocturnal mammals suggests that target-based spectral tuning may be occurring. In diurnal terrestrial animals, cone spectral tuning is often related to detecting targets against background radiance (such as red fruit against green foliage: Sumner and Mollon, 2000), and not irradiance directly (Fleishman et al., 1997; Leal and Fleishman, 2002; Osorio and Vorobyev, 2005). Furthermore, in diurnal aquatic animals, the variation in the SWS cones is often linked to target detection as well (McFarland and Munz, 1975; Cummings, 2007).

Whether this target detection in nocturnal mammals is mediated via an achromatic or chromatic channel is entirely unclear. Nocturnal color vision has been documented in frogs

(Gomez et al., 2010), geckos (Roth and Kelber, 2004), and insects (Kelber et al., 2002; Somanathan et al., 2008), however, its feasibility among mammals is still hotly debated. Some researchers suggest that color discrimination at night may be a physiological reality for certain species (Perry et al., 2007; Warrant, 2008; Müller et al., 2009; Zhao et al., 2009a; Zhao et al., 2009b; Melin et al., 2012), whereas others view it as unlikely (Ahnelt and Kolb, 2000; Wang et al., 2004). Although the understory of closed canopy rainforests is likely too dim for color vision at night (particularly at smaller lunar phases and low lunar altitude), the higher nocturnal light intensities available in more open canopy habitats/microhabitats (Table S4) may be bright enough to permit nocturnal color vision. Interestingly, both diurnal humans and arrhythmic horses can make color discriminations in moonlight, despite lacking nocturnal visual systems (Roth et al., 2008), suggesting that nocturnally-adapted mammals may have similar abilities (at least at moonlight levels). Under nearly all conditions in forests and woodlands, nocturnal light environments exhibited a general yellow-green peak flux. However, lunar altitude, lunar phase and canopy openness all substantially influenced the intensity of nocturnal light environments as well as the availability of shorter and longer wavelengths. Nocturnal animals thus encounter changing visual environments at temporal and spatial scales, particularly in seasonally deciduous forests. Kelber and colleagues have recently argued that nocturnal color vision may be advantageous in changing light environments in some nocturnal vertebrates (Kelber et al., 2002; Kelber et al., 2003; Johnsen et al., 2006; Kelber and Roth, 2006; Kelber and Lind, 2010; Kelber and Osorio, 2010). Similar arguments for the selective advantage of using color vision rather than achromatic cues in conditions that exhibit great spatial and temporal fluctuations in intensity have been made for terrestrial forests (Mollon, 1989) and aquatic forests (Cummings, 2004) in diurnal conditions. While the achromatic contrast of a target against a green leaf background can change dramatically under different illuminants, the chromatic contrast is much less variable and permits more reliable object discrimination (Mollon, 1989; Cummings, 2004; Johnsen et al., 2006). The results of our study of nocturnal light in forests confirm that nocturnal light environments can change rapidly (Johnsen et al., 2006), not only as the moon rises and sets, but as it travels across the sky.

Conclusions

Although many studies have investigated the spectral composition of irradiance in diurnal and twilight conditions (Munz and McFarland, 1973; Lythgoe, 1979; Endler, 1991; Endler, 1993;

Johnsen et al., 2006), very few have examined nocturnal light. Thus, this study offers the first comprehensive examination of the color of light in nocturnal forests and woodlands. While lunar phase and canopy openness were important predictors of nocturnal light environment, we found that the height of the moon in the sky had one of the strongest effects on both the intensity and spectral quality of nocturnal irradiance. In contrast to diurnal conditions, the much lower intensity of nocturnal light sources resulted in a yellow-green-rich nocturnal light environment that was generally constant across lunar phase, lunar altitude, microhabitat, and habitat type. However, we also identified temporal and spatial variation in light intensity and the availability of shorter and longer wavelengths within this general *nocturnal forest* light environment. We propose that this variation may have important implications for nocturnal vision and the appearance of visual targets. A metanalysis of visual pigments in nocturnal mammals suggests that LWS visual pigments may be tuned to maximize photon absorption in nocturnal light environments. Further, we found that fruit/flower detection may be involved in SWS spectral tuning. The results of this study suggest that nocturnal light environments and ecology may offer fertile ground for exploring variation in nocturnal visual systems, even within nocturnal mammals.

LIST OF SYMBOLS AND ABBREVIATIONS

Anko – Ankoasifaka Research Station, Kirindy Mitea National Park, Madagascar

Tala – Talatakely, Ranomafana National Park, Madagascar

Valo – Valohoaka, Ranomafana National Park, Madagascar

μM – micromoles (photometric unit: $\mu M/m^2/s/nm$)

AIC – Akaike Information Criterion

PGLS – phylogenetic generalized least squares

%SW - Percent short wavelength irradiance measured with filters (400-460 nm)

%MW –Percent middle wavelength irradiance measured with filters (490-540 nm)

%LW – Percent long wavelength irradiance measured with filters (560-650/680 nm)

λ_{max} – peak spectral sensitivity of visual pigment

SWS –short-wavelength-sensitive cones

LWS –long-wavelength-sensitive cones

ACKNOWLEDGEMENTS

We would like to thank C. Kirk, R. Lewis, L. Shapiro, D. Bolnick, G. Russo and two anonymous reviewers for advice and comments on previous versions of this manuscript. We also thank N. Marti of the UT Division of Statistics and Scientific Computation, A. Kemp and C. Scarry for statistical advice. Additionally, we are grateful to the Malagasy government and Madagascar National Parks for permitting CCV to conduct this study. We are also grateful to MICET, ICTE, and the staff at Centre ValBio and Kirindy Mitea for facilitating this project and the research assistants who helped collect data: RAKOTOSOLOFO Andrianandrasanarivelo, Reziky Clement, Birevotra Faharoy, Géorges RAZAFINDRAKOTO, AimeNoel NDRIATAHINA, Jean Baptiste VELONTSARA.

FUNDING

Funding for the project was provided by The Leakey Foundation (to CCV), The Wenner-Gren Foundation for Anthropological Research (7993 to CCV), The American Philosophical Society (Lewis and Clark Fund for Exploration and Field Research to CCV) and The American Society of Mammalogists (to CCV).

REFERENCES

Ahnelt, P. K. and Kolb, H. (2000). The mammalian photoreceptor mosaic-adaptive design. *Prog. Retin. Eye Res.* **19**, 711-777.

Baayen, R. H. (2010). languageR: Data sets and functions with "Analyzing Linguistic Data: A practical introduction to statistics." R package version 1.0. http://CRAN.R project.org/package=languageR.

Balko, E. A. and Underwood, B. H. (2005). Effects of forest structure and composition on food availability for *Varecia variegata* at Ranomafana National Park, Madagascar. *Am. J. Primatol.* **66**, 45-70.

Barlow, H. B., Levick, W. R. and Yoon, M. (1971). Responses to single quanta of light in retinal ganglion cells of the cat. *Vision Res.* **11**, 87-101.

Bates, D. and Maechler, M. (2010). lme4: Linear mixed-effects models using S4 classes. R package version 0.999375-37. http://CRAN.R-project.org/package=lme4.

Bidlingmayer, W. L. (1964). The effect of moonlight on the flight activity of mosquitoes. *Ecology* **45**, 87-94.

Bininda-Emonds, O. R. P., Cardillo, M., Jones, K. E., MacPhee, R. D. E., Beck, R. M. D., Grenyer, R., Price, S. A., Vos, R. A., Glittleman, J. L. and Purvis A. (2007). The delayed rise of present-day mammals. *Nature* **446**, 507-512.

Bowmaker, J. K., Govardovskii, V. I., Shukolyukov, S. A., L.V. Zueva, J., Hunt, D. M., Sideleva, V. G. and Smirnova, O. G. (1994). Visual pigments and the photic environment: the cottoid fish of Lake Baikal. *Vision Res.* **34**, 591-605.

Burgess, N. D., D'Amico Hales J., Underwood E. C., Dinerstein, E., Olson, D., Itoua, I., Schipper, J., Rickets, T. H. and Newman, K. (2004). *Terrestrial Ecoregions of Africa and Madagascar: A Conservation Assessment*. Washington, DC: Island Press.

Burnham, K. P. and Anderson D. R. (2002). *Model Selection and Multimodel Inference*, 2nd edition. New York, NY: Springer.

Burnham, K. P and Anderson, D. R. (2004). Multimodel inference: understanding AIC and BIC in model selection. *Sociol. Methods Res.* **33,** 261-304.

Burnham, K. P., Anderson, D. R. and Huyvaert K. P. (2011). AIC model selection and multimodel inference in behavioral ecology: some background, observations, and comparisons. *Behav. Ecol. Sociobiol.* **65**, 23-25.

Chiao, C. C., Vorobyev, M., Cronin T. W. and Osorio, D. (2000). Spectral tuning of dichromats to natural scenes. *Vision Res.* **40**, 3257-3271.

Condit, H. R. and Grum, F. (1964). Spectral energy distribution of daylight. *J. Opt. Soc. Am.* **54**, 937-940.

Cowing, J. A., Arrese, C. A., Davies, W. L., Beazley, L. D. and Hunt, D. M. (2008). Cone visual pigments in two marsupial species: the fat-tailed dunnart (*Sminthopsis crassicaudata*) and the honey possum (*Tarsipes rostratus*). *Proc. R. Soc. Lond. B Biol. Sci.* **275**, 1491-1499.

Cummings, M. E. (2007). Sensory trade-offs predict signal divergence in surfperch. *Evolution* **61**, 530-545.

Cummings, M. E. (2004). Modelling divergence in luminance and chromatic detection performance across measured divergence in surfperch (Embiotocidae) habitats. *Vision Res.* **44**, 1127-1145.

Cummings, M. E. and Partridge, J. C. (2001). Visual pigments and optical habitats of surfperch (Embiotocidae) in the California kelp forest. *J. Comp. Physiol. A* **187**, 875-889.

Cummings, M. E., Bernal, X. E., Reynaga, R., Rand, A. S. and Ryan, M. J. (2008). Visual sensitivity to a conspicuous male cue varies by reproductive state in *Physalaemus pustulosus* females. *J. Exp. Biol.* **211**, 1203-1210.

Endler, J. A. (1990). On the measurement and classification of color in studies of animal color patterns. *Biol. J. Linn. Soc. Lond.* **41**, 315-352.

Endler, J. A. (1991). Variation in the appearance of guppy color patterns to guppies and their predators under different visual conditions. *Vision Res.* **31**, 587-608.

Endler, J. A. (1993). The color of light in forests and its implications. *Ecol. Monogr.* **63**, 2-27.

Endler, J. A. and Thery, M. (1996). Interacting effects of lek placement, display behaviour, ambient light, and color patterns in three Neotropical forest-dwelling birds. *Am. Nat.* **148**, 421-452.

Fietz, J. and Ganzhorn, J. U. (1999). Feeding ecology of the hibernating primate *Cheirogaleus medius*: how does it get so fat? *Oecologia*, **121**, 157-164.

Fleishman, L. J., Bowman, M., Saunders, D., Miller, W. E., Rury, M. J. and Loew, E. R. (1997). The visual ecology of Puerto Rican anoline lizards: habitat light and spectral sensitivity. *J. Comp. Physiol. A* **181**, 446-460.

Frazer, G.W., Canham, C.D. and Lertzman, K.P. (1999). Gap Light Analyzer (GLA), Version 2.0: Imaging software to extract canopy structure and gap light transmission indices from true-color fisheye photographs, users manual and program documentation. Simon Fraser University, Burnaby, British Columbia, and the Institute of Ecosystem Studies, Millbrook, New York.

Garland, T. and Ives A. R. (2000). Using the past to predict the present: confidence intervals for regression equations in phylogenetic comparative methods. *Am. Nat.* **155**, 346-364.

Gomez, D., Richardson, C., Lengagne, T., Plenet, S., Joly, P., Léna, J.-P. and Théry, M. (2009). The role of nocturnal vision in mate choice: females prefer conspicuous males in the European tree frog (*Hyla arborea). Proc. R. Soc. Lond. B Biol. Sci.* **276**, 2351-2358.

Gomez, D., Richardson, C., Lengagne, T., Derex, M., Plenet, S., Joly, P., Léna, J.-P. and Théry, M. (2010). Support for a role of color vision in mate choice in the nocturnal European treefrog (*Hyla arborea*). *Behaviour* **147**, 1753-1768.

Harmon, L. J., Weir, J. T., Brock, C. D., Glor, R. E. and Challenger, W. (2008). GEIGER: investigating evolutionary radiations. *Bioinformatics* **24**, 129-131.

Hunt, D. M., Carvalho, L. S., Cowing, J. A., and Davies, W. L. (2009). Evolution and spectral tuning of visual pigments in birds and mammals. *Philos. Trans. R. Soc. Lond. B Biol. Sci.* **364**, 2941 -2955.

Jacobs, G. H. (2009). Evolution of colour vision in mammals. *Philos. Trans. R. Soc. B Biol. Sci.* **364**, 2957-2967.

Jacobs, G. H. and Rowe, M. P. (2004). Evolution of vertebrate colour vision. *Clin. Exp. Optom.* **87**, 206-216.

Johnsen, S. (2012). *The Optics of Life: A Biologist's Guide to Light in Nature*. Princeton, NJ: Princeton University Press.

Johnsen, S., Kelber, A., Warrant, E., Sweeney, A. M., Widder, E. A., Lee, R. L. and Hernandez-Andres, J. (2006). Crepuscular and nocturnal illumination and its effects on color perception by the nocturnal hawkmoth *Deilephila elpenor*. *J. Exp. Biol*. **209**, 789-800.

Kamilar, J. M., Muldoon, K. M., Lehman, S. M. and Herrera, J. P. (2012). Testing Bergmann's rule and the resource seasonality hypothesis in Malagasy primates using GIS-based climate data. *Am. J. Phys. Anthropol.* **147**, 401-408.

Kawamura, S. and Kubotera, N. (2004). Ancestral loss of short wave-sensitive cone visual pigment in lorisiform prosimians, contrasting with its strict conservation in other prosimians. *J. Mol. Evol.* **58**, 314-321.

Kelber, A., Balkenius, A. and Warrant, E. J. (2002). Scotopic color vision in nocturnal hawkmoths. *Nature* **419**, 922-925.

Kelber, A., Balkenius, A. and Warrant, E. J. (2003). Color vision in diurnal and nocturnal hawkmoths. *Int. Comp. Biol.* **43**, 571-579.

Kelber, A. and Roth, L. S. V. (2006). Nocturnal color vision□: not as rare as we might think. *J. Exp. Biol*. **209**, 781-788.

Kelber, A. and Lind, O. (2010). Limits of color vision in dim light. *Ophthalmic Physiol. Opt.* **30**, 454-459.

Kelber, A. and Osorio, D. (2010). From spectral information to animal color vision: experiments and concepts. *Proc. R. Soc. B Biol. Sci.* **277**, 1617-1625.

690 **Kieffer, H. H. and Stone T. C.** (2005). The spectral irradiance of the moon. *Astron. J.* **129**,
691 2887-2901.
692 **Lane, A.** P. and Irvine, W. M. (1973). Monochromatic phase curves and albedos for the lunar
693 disk. *Astron. J.* **78**, 267-277.
694 **Leal, M. and Fleishman, L. J.** (2002). Evidence for habitat partitioning based on adaptation to
695 environmental light in a pair of sympatric lizard species. *Proc. R. Soc. Lond. B Biol. Sci.*
696 **269**, 351-359.
697 **Lee, R. L., Jr and Hernández-Andrés, J.** (2003). Measuring and modeling twilight's purple
698 light. *Appl. Opt.* **42**, 445-457.
699 **Levine, J. S. and MacNichol E. F.** (1979). Visual pigments in teleost fishes: effects of habitat,
700 microhabitat, and behavior on visual system evolution. *Sens. Processes* **3**, 95-131.
701 **Lewis, R. J. and Bannar-Martin, K. H.** (2012). The impact of cyclone Fanele on a tropical dry
702 forest in Madagascar. *Biotropica* **44**, 135-140.
703 **Lillywhite, P. G.** (1977). Single photon signals and transduction in an insect eye. *J. Comp.*
704 *Physiol.* **122**, 189-200.
705 **Lukáts, A., Dkhissi-Benyahya, O., Szepessy, Z., Röhlich, P., Vígh, B., Bennett, N. C.,**
706 **Cooper, H. M., and Szél, A.** (2002). Visual pigment coexpression in all cones of two
707 rodents, the Siberian hamster, and the pouched mouse. *Invest. Ophthalmol. Vis. Sci*, **43**,
708 2468-2473.
709 **Lythgoe, J. N.** (1972). The adaptation of visual pigments to the photic environment. In
710 *Handbook of Sensory Physiology Vol. VII/1: Photochemistry of Vision* (ed. H. J. A.
711 Dartnall), pp. 566-603. New York: Springer-Verlag.
712 **Lythgoe, J. N.** (1979). *The Ecology of Vision.* Oxford: Clarendon Press.
713 **Lythgoe, J. N.** (1984). Visual pigments and environmental light. *Vision Res.* **24**, 1539-1550.
714 **Martin, G.** (1990). *Birds By Night.* London: Poyser.
715 **McFarland, W. N. and Munz, F. W.** (1975). Part III: the evolution of photopic visual pigments
716 in fishes. *Vision Res.* **15**, 1071-1080.
717 **Melin, A. D., Moritze, G. L., Fosbury, R. A. E., Kawamura S. and Dominy N. J.** (2012).
718 Why aye-ayes see blue. *Am. J. Primatol.* **74**, 185-192.

Miller, S. D. and Turner R. E. (2009). A dynamic lunar spectral irradiance data set for NPOESS/VIIRS day/night band nighttime environmental applications. *IEEE Trans. Geosci. Remote Sens.* **47**, 2316-2329.

Mollon, J. D. (1989). "Tho' she kneel'd in that place where they grew…" The uses and origins of primate colour vision. *J. Exp. Biol.* **146**, 21-38.

Müller, B., Glösmann, M., Peichl, L., Knop, G. C., Hagemann, C. and Ammermüller, J. (2009). Bat eyes have ultraviolet-sensitive cone photoreceptors. *PLoS ONE*, **4**, e6390.

Munz, F. W. and McFarland, W. N. (1973). The significance of spectral position in the rhodopsins of tropical marine fishes. *Vision Res*. **13**, 1829-1874.

Munz, F. W. and McFarland, W. N. (1977). Evolutionary adaptations of fishes to the photic environment. In *The Visual System of Vertebrates* (ed. F. Crescitelli), pp. 194-274. New York: Springer-Verlag.

Orme, D., Freckleton, R., Thomas, G., Petzoldt, T., Fritz, S. and Isaac, N. (2010). caper: comparative analyses of phylogenetics and evolution in R. R package version 0.4/r71. see http://www.R-Forge.R-project.org/projects/caper/.

Osorio, D. and Vorobyev, M. (2005). Photoreceptor spectral sensitivities in terrestrial animals: adaptations for luminance and colour vision. *Proc. R. Soc. Lond. B Biol. Sci.* **272**, 1745-1752.

Pagel, M. (1999). Inferring the historical patterns of biological evolution. *Nature* **401**, 877-884.

Paradis, E., Claude, J. and Strimmer, K. (2004). APE: analyses of phylogenetics and evolution in R language. *Bioinformatics* **20**, 287-290.

Pariente, G. F. (1980). Quantitative and qualitative study of the light available in the natural biotope of Malagasy prosimians. In *Nocturnal Malagasy Primates: Ecology, Physiology, and Behaviour* (eds. P. Charles-Dominique, H. M. Cooper, A. Hladik, C. M. Hladik, G. F. Pariente, A. Petter-Rousseaux, and A. Schilling), pp. 117-134.

Partridge, J. C. and Cummings, M. E. (1999). Adaptation of visual pigments to the aquatic environment. In, *Adaptive Mechanisms in the Ecology of* Vision (eds S. N. Archer, M. B. A. Djamgoz, E. R. Loew, J. C. Partridge and S. Vallerga), pp. 251-283. Boston: Kluwer Academic Publishers.

Perry, G. H., Martin, R. D. and Verrelli, B. C. (2007). Signatures of functional constraint at aye-aye opsin genes: the potential of adaptive color vision in a nocturnal primate. *Mol. Biol. Evol.* **24**, 1963-1970.

R Development Core Team (2011). R: A language and environment for statistical computing. R Foundation for Statistical Computing, Vienna, Austria. ISBN 3-900051-07-0, URL http://www.R-project.org/.

Roth, L. S. V. and Kelber, A. (2004). Nocturnal color vision in geckos. *Proc. R. Soc. Lond. B Biol. Sci.* **271**, S485-S487.

Shaw, J. A. (2005). The digital blue sky at night. *Opt. Photonics News* **16**, 18-23.

Somanathan, H., Borges, R. M., Warrant, E, J. and Kelber, A. (2008). Nocturnal bees learn landmark colors in starlight. *Curr. Biol.* **18**, R996-R997.

Sorg, J.-P. and Rohner, U. (1996). Climate and tree phenology of the dry deciduous forest of the Kirindy Forest. *Primate Report* **46-1**, 57-80.

Sumner, P. and Mollon, J. D. (2000). Catarrhine photopigments are optimized for detecting targets against a foliage background. *J. Exp. Biol.* **203**, 1963-1986.

Sweeney, A. M., Boch, C. A., Johnsen, S. and Morse, D. E. (2011). Twilight spectral dynamics and the coral reef invertebrate spawning response. *J. Exp. Biol.* **214**, 770-777.

Symonds M. R. E. and Moussalli A. (2011). A brief guide to model selection, multimodel inference and model averaging in behavioural ecology using Akaike's information criterion. *Behav. Ecol. Sociobiol.* **65**, 13-21.

Théry, M. (2001). Forest light and its influence on habitat selection. *Plant Ecol.* **153**, 251-261.

Umino, Y., Solessio, E. and Barlow R. B. (2008). Speed, spatial, and temporal tuning of rod and cone vision in mouse. *J. Neurosci.* **28**, 189-198.

United States Navy (1952). Natural Illumination Charts. United States Navy Research and Development project NS 714-100. Report No. 374-1 (September).

United States Naval Observatory (2011). Complete sun and moon data for one day. *Astronomical Applications Department, United States Navy*, http://aa.usno.navy.mil/data/docs/RS_OneDay.php (November 27, 2011).

Walls, G. L. (1942). *The Vertebrate Eye and Its Adaptive Radiation*. Bloomfield Hills, Michigan: The Cranbrook Press.

Wang, D., Oakley, T., Mower, J., Shimmin, L. C., Yim, S., Honeycutt, R. L., Tsao, H. and Li, W.-H. (2004). Molecular evolution of bat color vision genes. *Mol. Biol. Evol.* **21**, 295-302.

Warrant, E. J. (2004). Vision in the dimmest habitats on Earth. *J. Comp. Physiol. A* **190**, 765-789.

Warrant, E. J. (2008). Nocturnal vision. In *The Senses: A Comprehensive Reference Vol. 2: Vision II* (eds. T. Albright, and R. H. Masland), pp. 53-86. Oxford: Academic Press.

Wright, P. C. (1992). Primate ecology, rainforest conservation, and economic development: building a national park in Madagascar. *Evol. Anthropol.* **1**, 25-33.

Young, R. E. and Mencher F., M. (1980). Bioluminescence in mesopelagic squid: diel color change during counterillumination. *Science* **208**, 1286-1288.

Zhao, H., Rossiter, S. J., Teeling, E. C., Li, C., Cotton, J. A. and Zhang, S. (2009a). The evolution of color vision in nocturnal mammals. *Proc. Natl. Acad. Sci. U S A* **106**, 8980-8985.

Zhao, H., Xu, D., Zhou, Y., Flanders, J. and Zhang, S. (2009b). Evolution of opsin genes reveals a functional role of vision in the echolocating little brown bat (*Myotis lucifugus*). *Biochem. Syst. Ecol.* **37**, 154-161.

Zuur, A. F., Ieno, E. N., Walker, N. J., Saveliev, A. A. and Smith, G. M. (2009). *Mixed Effects Models and Extensions in Ecology with R.* New York: Springer.

FIGURE LEGENDS

Fig. 1. Lunar phase and nocturnal irradiance spectra from the seasonally dry deciduous forest/woodland at Anko during the dry season (July-September, 2009). Points indicate mean irradiance values (**A, B**) or mean normalized values (**C**) for each narrow bandpass interference filter and bars indicate standard error. (**A)** and (**B)** Irradiance spectra in clear night sky at Anko for all lunar altitudes. (**B**) Subset of data (crescent and no moon) from **A** at a lower range of Y-axis values. Data for **A** and **B**: full moon (n=117), gibbous moon (n=39), quarter moon (n=20), crescent moon (n=8), and no moon (n=105). (**C**) Mean and standard deviation of normalized nocturnal irradiance spectra by lunar phase with the moon at 30-59.9° altitude in clear sky. Data: full moon (n=68), quarter moon (n=15), no moon present (n=105).

Fig. 2. Effects of lunar altitude and nocturnal irradiance spectra at Anko under full moonlight in clear sky. Points indicate mean irradiance values (**A**) or mean normalized values (**B**) for each narrow bandpass interference filter and bars indicate standard error. (**A**) Log-transformed irradiance spectra at different lunar altitudes. (**B**) Effects of lunar altitude on normalized nocturnal spectra. Data: 0-29.9° (*n*=14), 30-59.9° (*n*=68), 60-90° (*n*=35).

Fig. 3. Effects of canopy openness on nocturnal irradiance spectra at Anko under full moonlight and starlight in clear sky. Points indicate mean irradiance values (**A-C**) or mean normalized values (**D-E**) for each narrow bandpass interference filter and bars indicate standard error. (**A**) and (**D**) Effects of canopy openness on nocturnal irradiance in full moonlight at higher lunar altitudes (>45°) for absolute and normalized irradiance, respectively. Data: <30% (*n*=8), 30-44.9% (*n*=47), 45%+ (*n*=10). (**B**) and (**E**) Effects of canopy openness on nocturnal irradiance in full moonlight at lower lunar altitudes (< 45°) for absolute and normalized irradiance, respectively. Data: <30% (*n*=8), 30-45% (*n*=29), 45%+ (*n*=10). (**C**) and (**F**) Effects of canopy openness on nocturnal irradiance when no moon was present for absolute and normalized irradiance, respectively. Data: <30% (*n*=8), 30-39% (*n*=53), 40%+ (*n*=38).

Fig. 4. Predicted and observed values (*n*=242) for absolute total flux and relative flux by different bandwidths (%SW: 400-460 nm; %MW: 490-540 nm; %LW: 560-680 nm) based on best-fit linear mixed models. Correlation coefficient, degrees of freedom, and *p*-values provided for predicted *vs.* observed values from the Anko dry forest dataset (black circles). Dashed line in each panel depicts expectations under a one-to-one relationship (slope=1, intercept=0) between predicted and observed values. Red stars are predicted and observed values for rainforest data fit to the dry forest linear model. Model parameters, including slopes and intercepts, are provided in Table S3, and equations in text. (**A**) Log total flux, (**B**) %SW (400-460 nm), (**C**) %MW (490-540 nm) and (**D**) %LW (560-680 nm).

Fig. 5. Nocturnal irradiance comparisons between the dry forest at Anko and the rainforest at Valo and Tala. Comparative Anko spectra were only available from more open canopy microhabitats (> 37% canopy openness). Points indicate mean irradiance values (**A**, **B**) or normalized values (**C**, **D**) for each narrow bandpass interference filter and bars indicate standard

error. (**A**) and (**C**) Nocturnal light in crescent moonlight (lunar altitude 6.4-28.5°) in clear sky at Valo (*n*=8) and Anko (*n*=8) for absolute and normalized irradiance, respectively. (**B**) and (**D**) Nocturnal light in gibbous moonlight (lunar altitude 30.4-56°) in cloudy sky at Tala (*n*=6) and Anko (*n*=14) for absolute and normalized irradiance, respectively.

Fig. 6. Visual pigment peak spectral sensitivity in **(A**) nocturnal mammals and (**B**) other nocturnal vertebrates based on published data (Table S1). For (A), mammal species in bold and with shaded lines are fruit/flower consumers. Closed circles=SWS cones, asterisks=rods, open circles=LWS cones. Solid lines represent loss of SWS cones.

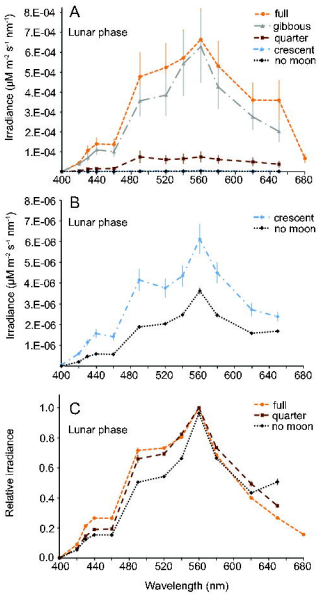
A
Lunar phase
full
gibbous
quarter
crescent
no moon
Irradiance (μM m⁻² s⁻¹ nm⁻¹)
8.E-04
7.E-04
6.E-04
5.E-04
4.E-04
3.E-04
2.E-04
1.E-04
400
440
480
520
560
600
640
680
B
Lunar phase
crescent
no moon
Irradiance (μM m⁻² s⁻¹ nm⁻¹)
8.E-06
7.E-06
6.E-06
5.E-06
4.E-06
3.E-06
2.E-06
1.E-06
C
Lunar phase
full
quarter
no moon
Relative irradiance
1.0
0.8
0.6
0.4
0.2
0.0
Wavelength (nm)

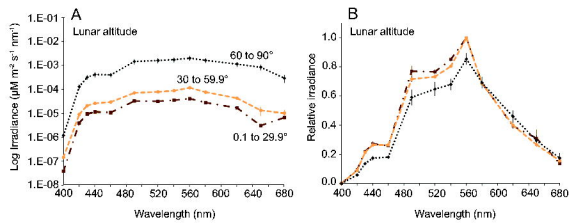
A
Lunar altitude
60 to 90°
30 to 59.9°
0.1 to 29.9°
Log Irradiance (µM m⁻² s⁻¹ nm⁻¹)
1.E-01
1.E-02
1.E-03
1.E-04
1.E-05
1.E-06
1.E-07
1.E-08
400
440
480
520
560
600
640
680
Wavelength (nm)
B
Lunar altitude
Relative Irradiance
1.0
0.8
0.6
0.4
0.2
0.0
400
440
480
520
560
600
640
680
Wavelength (nm)

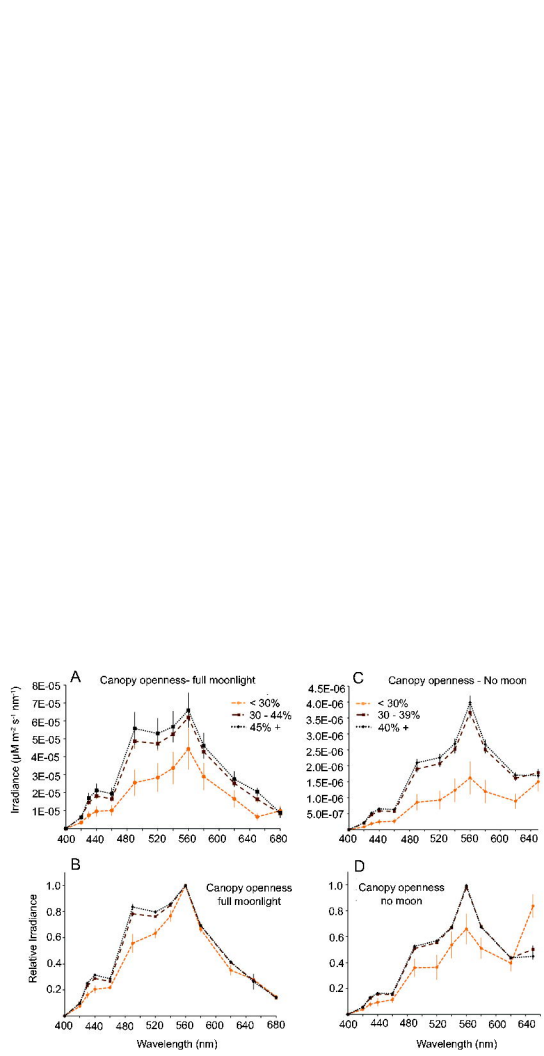
A
Canopy openness- full moonlight
< 30%
30 - 44%
45% +
Irradiance (µM m⁻² s⁻¹ nm⁻¹)
8E-05
7E-05
6E-05
5E-05
4E-05
3E-05
2E-05
1E-05
400 440 480 520 560 600 640 680
C
Canopy openness - No moon
< 30%
30 - 39%
40% +
4.5E-06
4.0E-06
3.5E-06
3.0E-06
2.5E-06
2.0E-06
1.5E-06
1.0E-06
5.0E-07
400 440 480 520 560 600 640
B
Canopy openness
full moonlight
Relative Irradiance
1.0
0.8
0.6
0.4
0.2
400 440 480 520 560 600 640 680
Wavelength (nm)
D
Canopy openness
no moon
1.0
0.8
0.6
0.4
0.2
400 440 480 520 560 600 640
Wavelength (nm)

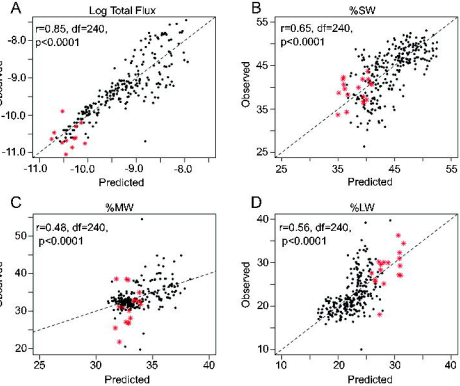
A
Log Total Flux
r=0.85, df=240,
p<0.0001
Observed
Predicted
-8.0
-9.0
-10.0
-11.0
B
%SW
r=0.65, df=240,
p<0.0001
Observed
Predicted
25
35
45
55
C
%MW
r=0.48, df=240,
p<0.0001
Observed
Predicted
20
30
40
50
D
%LW
r=0.56, df=240,
p<0.0001
Observed
Predicted
10
20
30
40

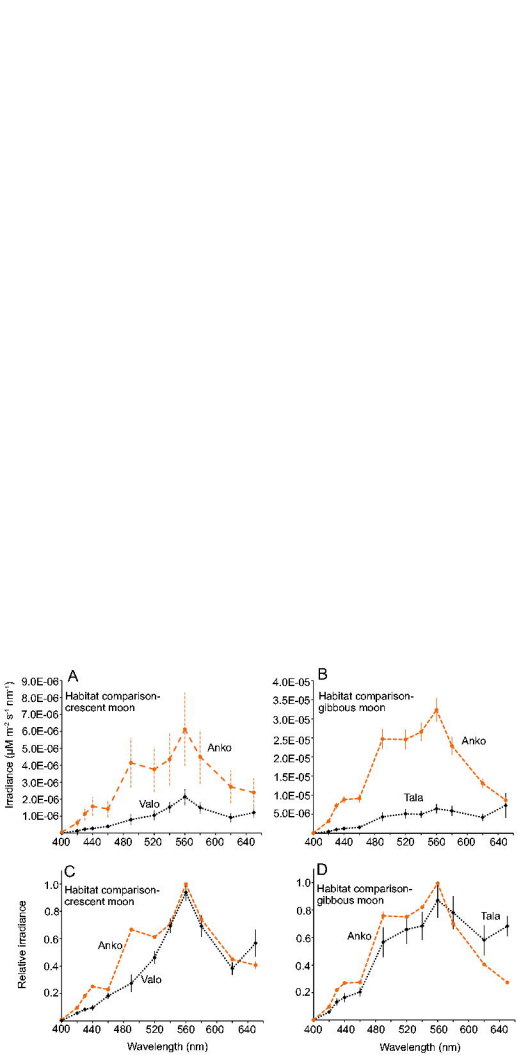
A
Habitat comparison-
crescent moon
Anko
Valo
B
Habitat comparison-
gibbous moon
Anko
Tala
C
Habitat comparison-
crescent moon
Anko
Valo
D
Habitat comparison-
gibbous moon
Anko
Tala
Irradiance (μM m⁻² s⁻¹ nm⁻¹)
Relative Irradiance
Wavelength (nm)
Wavelength (nm)

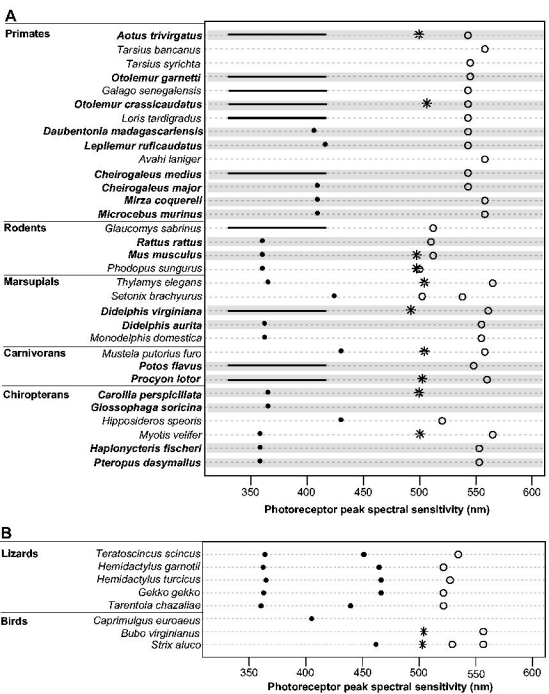
A
Primates
Aotus trivirgatus
Tarsius bancanus
Tarsius syrichta
Otolemur garnetti
Galago senegalensis
Otolemur crassicaudatus
Loris tardigradus
Daubentonia madagascariensis
Lepilemur ruficaudatus
Avahi laniger
Cheirogaleus medius
Cheirogaleus major
Mirza coquereli
Microcebus murinus
Rodents
Glaucomys sabrinus
Rattus rattus
Mus musculus
Phodopus sungurus
Marsupials
Thylamys elegans
Setonix brachyurus
Didelphis virginiana
Didelphis aurita
Monodelphis domestica
Carnivorans
Mustela putorius furo
Potos flavus
Procyon lotor
Chiropterans
Carollia perspicillata
Glossophaga soricina
Hipposideros speoris
Myotis velifer
Haplonycteris fischeri
Pteropus dasymallus
350
400
450
500
550
600
Photoreceptor peak spectral sensitivity (nm)
B
Lizards
Teratoscincus scincus
Hemidactylus garnotii
Hemidactylus turcicus
Gekko gekko
Tarentola chazaliae
Birds
Caprimulgus euroaeus
Bubo virginianus
Strix aluco
350
400
450
500
550
600
Photoreceptor peak spectral sensitivity (nm)

Table 1. Factor weights for linear mixed models.

Factor	Log Total Flux	%SW	%MW	%LW
Altitude	1.0000	1.0000	1.0000	1.0000
Phase	1.0000	1.0000	0.9960	1.0000
Canopy	0.9891	0.9998	0.7772	0.9998
Altitude * Phase	0.3695	1.0000	0.5899	1.0000
Altitude * Canopy	0.2811	0.9993	0.5073	0.9978
Phase * Canopy	0.3222	0.1193	0.6099	0.5002
Altitude * Phase * Canopy	0.0222	0.1191	0.3743	0.4989

Factor weight reflects probability that factor is present in the best model.
Notes: Altitude = cosine lunar altitude, Phase = lunar phase function, Canopy = fraction canopy openness. Spectral bandwidths: %SW (400-460 nm), %MW (490-540 nm), %LW (560-680 nm).

Table 2. Results of PGLS for effects of diet and habitat type on cone pigment spectral tuning.

	Slope	F-statistic (df)	*p*-value	r^2	Pagel's Lambda
SWS					
Fruit/flowers (13Y, 4N)	**-40.08**	**9.934 (2,15)**	**0.002**	**0.398**	**1.00**
Habitat (7 open, 3 closed)	6.014	0.246 (2,8)	0.788	0.030	1.00
LWS					
Fruit/flowers (18Y, 11N)	3.131	0.250 (2,27)	0.781	0.009	0.72
Habitat (8 open, 8 closed)	2.375	0.412 (2,14)	0.670	0.029	0.00

Bold represents significant effect. Sample sizes for each analysis in parentheses.
Fruit/flowers = whether fruit or flower products are >10% of a species' diet.
Habitat = open canopy woodland/forest *vs.* closed canopy forest